

# Wavelet Constrained Regularization For Disparity Map Estimation

Wided Miled, Jean-Christophe Pesquet, Michel Parent

► **To cite this version:**

Wided Miled, Jean-Christophe Pesquet, Michel Parent. Wavelet Constrained Regularization For Disparity Map Estimation. European Signal Processing Conference, Sep 2006, Florence - Italy. inria-00001256v3

**HAL Id: inria-00001256**

**<https://hal.inria.fr/inria-00001256v3>**

Submitted on 16 May 2006

**HAL** is a multi-disciplinary open access archive for the deposit and dissemination of scientific research documents, whether they are published or not. The documents may come from teaching and research institutions in France or abroad, or from public or private research centers.

L'archive ouverte pluridisciplinaire **HAL**, est destinée au dépôt et à la diffusion de documents scientifiques de niveau recherche, publiés ou non, émanant des établissements d'enseignement et de recherche français ou étrangers, des laboratoires publics ou privés.

# WAVELET-CONSTRAINED REGULARIZATION FOR DISPARITY MAP ESTIMATION

Wided Miled<sup>1,2</sup>, Jean Christophe Pesquet<sup>2</sup> and Michel Parent<sup>1</sup>

<sup>1</sup>INRIA, IMARA Project  
Domaine de Voluceau  
78150 Le Chesnay, Cedex France  
email : {wided.miled,michel.parent}@inria.fr

<sup>2</sup>Institut Gaspard Monge / UMR-CNRS 8049  
Université Marne-la-Vallée, Champs-sur-Marne  
77454 Marne-la-Vallée, France  
e-mail: pesquet@univ-mlv.fr

## ABSTRACT

This paper describes a novel method for estimating dense disparity maps, based on wavelet representations. Within the proposed set theoretic framework, the stereo matching problem is formulated as a constrained optimization problem in which a quadratic objective function is minimized under multiple convex constraints. These constraints arise from the prior knowledge and the observations. In order to obtain a smooth disparity field, while preserving edges, we consider appropriate wavelet based regularization constraints. The resulting optimization problem is solved with a block iterative method which offers great flexibility in the incorporation of several constraints. Experimental results on both synthetic and real data sets show the excellent performance and robustness w.r.t. noise of our method.

## 1. INTRODUCTION

Stereo vision is a reliable technique for extracting 3D information of a scene from 2D images and it is effective for various tasks such as face recognition, autonomous navigation and view synthesis. One of the fundamental problems in stereo analysis is to establish a correspondence between a pair of left and right stereoscopic views. A great number of approaches for disparity map estimation have been proposed in the literature, including feature-based, area-based and energy-based approaches. A survey for the different approaches can be found in [1], [2]. In the feature-based techniques, the disparity is evaluated only for selected features extracted from the images, which leads to sparse disparity maps. Denser fields can be obtained by an area-based approach which attempts to determine the correspondence for each point visible in the stereo pair. The energy-based approach is mainly based on optimizing an energy function  $E$  which is the sum of a similarity term  $C$  and a smoothness term  $S$ :

$$E(u) = C(u) + \lambda S(u), \quad (1)$$

where  $u$  denotes the field to be estimated. The first term is the *intensity constancy* term, the second one is the *regularization* term, and  $\lambda > 0$  is a constant weighting the two terms. While these techniques achieve satisfactory results in certain situations, they are often implemented using numerical schemes which may be computationally intensive. Moreover, the choice of Lagrange parameter  $\lambda$  may be a difficult task.

Multiresolution representations as coarse-to-fine strategies have been developed aiming at reducing the computational complexity [3], [4], [5]. The related pyramidal structures allow to progressively build up finer disparity maps from coarser ones. However, pyramidal structures using Gaussian or Laplacian filters do not always have a good orientation selectivity [5].

Wavelet analysis have been shown to provide an appropriate way of performing a multi-scale analysis. In [4], a hierarchical stereo matching strategy using the Discrete Wavelet Transform (DWT) is proposed. The wavelet transform is used for its ability to extract salient features. Image components extracted from approximation and detail subbands of the decomposition are combined to compute the disparity at each level. Moreover, it has been demonstrated in [3] that coarse to fine wavelet-based strategies lead to a good recovery of large displacements.

Although the decomposition onto a wavelet basis has many desirable mathematical properties, it is not translation invariant in space. The lack of translation invariance means that a small shift in the samples of the input image may result in large changes in the wavelet coefficients, which ends up with variable results in image processing tasks. Representations with translation invariance characteristics are highly desirable for stereo vision and have been the focus of a lot of research [5].

This paper describes a new method for computing the disparity map, based on an analysis onto a wavelet frame. We first show that the stereo matching problem can be cast as a constrained optimization problem in which an appropriate objective function is minimized under certain convex constraints. In order to preserve field discontinuities while regularizing the solution, we construct an edge-preserving regularization constraint in the wavelet domain. Since wavelets provide a simple characterization of a wide variety of function smoothness spaces, the regularization constraint is defined as a (semi-)norm in an appropriate image space. The method presented here is inspired from a recent work that has proven to be very useful in some image processing tasks such as image restoration [6].

The organization of the paper is as follows. In Section 2, we describe our stereo model by formulating the matching problem as a constrained optimization problem. Section 3 is devoted to presenting the wavelet based regularization constraint. A numerical scheme to solve the resulting optimization problem is proposed in Section 4. Finally, we illustrate the proposed approach through experiments in Section 5. We conclude in Section 6.

## 2. PROBLEM FORMULATION

Given two intensity images  $I_L$  and  $I_R$ , taken from two parallel cameras so that corresponding epipolar lines lie on identical horizontal scanlines, the process of stereo matching is summarized as follows. From a 2D image point in the reference stereo image, we compute a confidence measure for each disparity within a search range  $\Omega$  and the disparity providing the minimum value is regarded as the optimal disparity value. Using the left image as the reference image, this matching problem can be formulated as

$$\hat{u}(x, y) = \arg \min_{u \in \Omega} \tilde{J}(I_L(x, y), I_R(x - u(x, y), y)), \quad (2)$$

where  $\hat{u}$  is the estimated disparity field,  $\Omega$  is the range of candidate disparity vectors and  $\tilde{J}$  is a cost function. For simplicity, the Sum of Squared Differences (SSD) is often used as a confidence measure :

$$\tilde{J}(u) = \sum_{(x,y) \in \mathcal{D}} [I_L(x,y) - I_R(x - u(x,y), y)]^2, \quad (3)$$

where  $\mathcal{D} \subset \mathbb{N}^2$  is the image support. Assuming that an initial estimate  $\bar{u}$  of  $u$  is available, for example from a previous estimation (possibly within an iterative process), and that the magnitude difference of the fields  $\hat{u}$  and  $\bar{u}$  is relatively small, we can approximate the warped right image around  $\bar{u}$  by a Taylor expansion as follows:

$$I_R(x - u, y) \simeq I_R(x - \bar{u}, y) - (u - \bar{u}) I_R^x(x - \bar{u}, y), \quad (4)$$

where  $I_R^x(x - \bar{u}, y)$  is the horizontal gradient of the warped right image. Note that for notation concision, we have not made explicit that  $u$  and  $\bar{u}$  are functions of  $(x, y)$  in the above expression.

Inserting the linearization (4) in (3), we end up with the following quadratic criterion:

$$J(u) = \sum_{(x,y) \in \mathcal{D}} [L(x, y) u - r(x, y)]^2, \quad (5)$$

where

$$L(x, y) = I_R^x(x - \bar{u}, y), \quad (6)$$

$$r(x, y) = I_R(x - \bar{u}, y) + \bar{u} L(x, y) - I_L(x, y). \quad (7)$$

Now, the goal is to estimate the disparity image  $u$  from the observed fields  $L$  and  $r$ . Inspired from approaches developed for image restoration purposes in [6], [7], this problem can be cast as a convex optimization problem. More precisely, a quadratic objective function is minimized under convex constraints. These constraints arise from the prior knowledge and the observed data and are represented by convex sets in the solution space. The minimization process is carried out over the feasibility set, which corresponds to the intersection of the constraint sets.

A general formulation of this problem in a Hilbert image space  $H$  is

$$\text{Find } u \in S = \bigcap_{i=1}^m S_i \text{ such that } J(u) = \inf J(S), \quad (8)$$

where the objective  $J : H \rightarrow ]-\infty, +\infty]$  is a convex function and the constraint sets  $(S_i)_{1 \leq i \leq m}$  are closed convex subsets of  $H$ . Constraint sets can generally be modelled as level sets:

$$\forall i \in \{1, \dots, m\}, \quad S_i = \{u \in H \mid f_i(u) \leq \delta_i\}, \quad (9)$$

where  $f_i : H \rightarrow ]-\infty, +\infty]$  is a convex functions and  $\delta_i \in \mathbb{R}$ .

Recently, there have been several attempts in formulating constraints in the wavelet domain [6], [8]. In fact, as shown in [6], convex wavelet constraints can be constructed and used with various spatial constraints to refine the feasibility set  $S$  in (8), yielding improved results for many image processing applications. In this paper, we investigate a new wavelet based edge preserving regularization constraint which is useful in disparity estimation problem.

### 3. WAVELET BASED REGULARIZATION CONSTRAINT

It is well-known that the stereo matching problem is an inverse ill-posed problem. Therefore, some constraints are required to regularize the solution. These constraints arise

from prior knowledge and rely on various properties of the field to be estimated. The smoothness constraint, originally introduced by Horn and Schunk [9], has been one of the most popular regularity assumptions. However, the *Tikhonov* quadratic term used to recover a smooth solution often introduces too much regularization, in particular resulting in oversmoothed edges. In disparity estimation, one would like to smooth isotropically inside homogeneous regions and preserve discontinuities around object edges. This can be achieved with the help of a suitable regularization constraint.

Recently, there have been many works on the formulation of edge-preserving regularization methods [12]. A recent advance in this area is the use of the Total Variation (TV) measure also related to the regularity class of functions with Bounded Variations (BV) [7], [11]. Controlling the TV amounts to smooth uniformly homogeneous regions while preserving sharp edges.

In the present work, we adopt an alternative wavelet domain approach to construct a regularization constraint based on image transformed coefficients. Our approach differs from existing wavelet-based disparity estimation methods as the key idea is to efficiently build the regularization constraint in the wavelet domain.

#### 3.1 Notation

Here, we only introduce the basic notation. For a comprehensive introduction to the wavelet theory, the reader is referred to [14]. The image space is the real Hilbert space  $H = L^2(\mathbb{R}^2)$ , with scalar product  $\langle \cdot | \cdot \rangle$  and norm  $\| \cdot \|$ . The 2-D wavelet transform in a separable wavelet basis  $\mathcal{B}$  is denoted by  $W^{\mathcal{B}}$ . The wavelet coefficients of  $u \in H$  are denoted by  $(w_{j,o,k}^{\mathcal{B}}(u))_{k \in \mathbb{Z}^2}$ , where  $o \in \{1, 2, 3\}$  is the orientation parameter and  $j \in \mathbb{Z}$  is the resolution level.  $T^*$  denotes the adjoint of a bounded linear operator  $T$  and the maximum resolution level is denoted by  $K$ .

#### 3.2 Wavelet regularization constraint

With the conventions above, we can represent a constraint function in the wavelet domain based on image coefficients as:

$$f_i = \varphi \circ W^{\mathcal{B}}, \quad (10)$$

where  $\varphi : H \mapsto ]-\infty, +\infty]$  is a convex function.

In order to deal with a regularization process that avoids smoothing across discontinuities, we have to consider a function  $\varphi$  that possesses particular smoothness characteristics. We propose here to use the norm of Besov spaces  $B_{p,q}^{\sigma}$ ,  $0 < \sigma < \infty$ ,  $1 \leq p, q \leq \infty$ , as they are appropriate to model images that contain discontinuities. The notion of Besov regularization has been introduced in the area of image denoising [6], [8] and has been shown to guarantee the requested smoothness properties. It is well-known that the Besov norm of an image  $u$  is equivalent to the following norm of its wavelet coefficients:

$$\|u\|_{B_{p,q}^{\sigma}} = \left( \sum_j \left( \sum_{k,o} 2^{j(\sigma p + p - 2)} |w_{j,o,k}^{\mathcal{B}}(u)|^p \right)^{q/p} \right)^{1/q}. \quad (11)$$

Various settings of the three parameters  $\sigma, p$  and  $q$  yield several members of the family of Besov spaces. One particular Besov space which plays an important role in image processing is when  $p = q$ . Then, the Besov norm reduces to a simple weighted  $p$ -norm of the wavelet coefficients. By further discarding the diagonal coefficients where noise often dominates, we obtain the following semi-norm:

$$f_i : u \mapsto \left( \sum_j \sum_{k \in \mathbb{Z}^2, o \in \{1,2\}} 2^{j(\sigma p + p - 2)} |w_{j,o,k}^{\mathcal{B}}(u)|^p \right)^{1/p}. \quad (12)$$

Motivated by the success of the space of functions of Bounded Variation that can efficiently model signals with sharp discontinuities, we will consider the space of minimal smoothness  $B_{1,1}^1$  by taking  $p = 1$  and  $\sigma = 1$ . This space is very close to the space BV since  $B_{1,1}^1 \subset \text{BV}$ . Imposing an upper bound  $\kappa_1$  on the (semi-)norm of this space restricts the solutions to the convex set:

$$S_1^{(0,0)} = \{u \in H \mid \sum_{j,k,o} |w_{j,o,k}^{\mathcal{B}}(u)| \leq \kappa_1\}, \quad (13)$$

where  $\kappa_1 > 0$ . Additionally, we propose to study another (semi-)norm which is mathematically equivalent to the previous one and therefore satisfies the properties of edge-preserving regularization. The convex set associated to this (semi-)norm, expressed in terms of the wavelet coefficients, is given by

$$S_2^{(0,0)} = \{u \in H \mid \sum_{j,k} (\sum_o |w_{j,o,k}^{\mathcal{B}}(u)|^2)^{1/2} \leq \kappa_2\}. \quad (14)$$

where  $\kappa_2 > 0$ . When Haar wavelets are used, it is worth noticing the similarity of the previous constraint with a discretized TV constraint.

To cope with the shift variance of the Discrete Wavelet Transform, that arises due to the decimation of a factor 2 in the decomposition process, we consider a shift-invariant wavelet representation [10]. This amounts to computing the wavelet coefficients of  $2^{2K}$  circular shifts of the original image. For limiting the computational complexity, rather than using a global smoothness constraint on the wavelet frame coefficients, we split this constraint into several constraints involving the (semi-)norms of the shifted image as expressed above. In other words, for the first regularity constraint, we have

$$S_1 = \bigcap_{s \in \{0, \dots, 2^K - 1\}^2} S_1^{(s)} \quad (15)$$

$$S_1^{(s)} = \{u \in H \mid \sum_{j,k,o} |w_{j,o,k}^{\mathcal{B}}(u^{(s)})| \leq \kappa_1\}, \quad (16)$$

where  $u^{(s)}$  is the shifted-by- $s$  image. Obviously, for  $s = (0,0)$ ,  $u^{(s)}$  is the original image  $u$  and  $S_1^{(s)}$  simply reduces to the convex set given in (13). The same strategy applies to the definition of the convex set  $S_2$  from the constraint (14).

Note that the upper bounds  $\kappa_1$  and  $\kappa_2$  can be estimated from experiments on available databases. We illustrate and compare the smoothness behaviors of the different (semi-)norms in Section 5.

## 4. NUMERICAL IMPLEMENTATION

### 4.1 Subgradient projections

Here, we briefly recall essential facts on convex analysis. Let  $S_i$  be the closed and convex subset of  $H$  given by (9), where  $f_i$  is a continuous and convex function. A vector  $t_i \in H$  is a subgradient of the convex function  $f_i$  at  $u \in H$  if

$$\forall v \in H, \quad \langle v - u \mid t_i \rangle + f_i(u) \leq f_i(v). \quad (17)$$

The set of all subgradients of  $f_i$  at  $u$  is the subdifferential of  $f_i$  at  $u$  and is denoted by  $\partial f_i(u)$ . Fix  $u \in H$  and a subgradient  $t_i \in \partial f_i(u)$ , the subgradient projection  $P_i u$  of  $u$  onto  $S_i$  is given by:

$$P_i u = \begin{cases} u - \frac{f_i(u) - \delta_i}{\|t_i\|^2} t_i, & \text{if } f_i(u) > \delta_i; \\ u, & \text{if } f_i(u) \leq \delta_i. \end{cases} \quad (18)$$

We note that computing  $P_i u$  is often a much simpler task than computing the exact projection onto  $S_i$ , as the latter amounts to solving a constrained minimization problem [13]. However, when the projection is easy to compute, one can use it as a subgradient projection.

Now suppose that  $\varphi$  is convex and that there exist a point  $u \in H$  such that  $\varphi$  is continuous at  $W^{\mathcal{B}}(u)$ . Then, for the constraint described in (10), we have:

$$\partial f_i(u) = (W^{\mathcal{B}})^* \partial \varphi(W^{\mathcal{B}}(u)), \quad (19)$$

where  $(W^{\mathcal{B}})^* = (W^{\mathcal{B}})^{-1}$  due to the orthonormality of the basis  $\mathcal{B}$ . For the constraint defined in (13), the expression of a subgradient projection can be deduced from [6].

### 4.2 Algorithm

We now proceed to the description of the block iterative algorithm proposed in [13] to solve the quadratic convex problem (8) which is equivalent to minimizing

$$u \mapsto \langle u - u_0, R(u - u_0) \rangle \quad (20)$$

over  $S$ , when  $R$  is a self-adjoint definite positive operator and  $u_0 \in H$ .

#### 4.2.1 Algorithm

1. Fix  $\varepsilon \in ]0, 1/m[$  and set  $n = 0$ .
2. Take a nonempty index set  $I_n \subseteq \{1, \dots, m\}$ .
3. For every  $i \in I_n$ , set  $a_{i,n} = P_{i,n} - u_n$  where  $P_{i,n}$  is a subgradient projection of  $u_n$  onto  $S_i$  as in (18).
4. Choose weights  $\{\xi_{i,n}\}_{i \in I_n} \subset ]\varepsilon, 1]$  such that  $\sum_{i \in I_n} \xi_{i,n} = 1$ .
  1. Set  $v_n = \sum_{i \in I_n} \xi_{i,n} a_{i,n}$  and  $L_n = \sum_{i \in I_n} \xi_{i,n} \|a_{i,n}\|^2$ .
5. If  $L_n = 0$ , exit iteration. Otherwise, set  $b_n = u_0 - u_n$ ,  $c_n = R b_n$ ,  $d_n = R^{-1} v_n$  and  $\tilde{L}_n = L_n / \langle d_n, v_n \rangle$ .
6. Choose  $\lambda_n \in [\varepsilon \tilde{L}_n, \tilde{L}_n]$  and set  $d_n = \lambda_n d_n$ .
7. Set  $\pi_n = -\langle c_n, d_n \rangle$ ,  $\mu_n = \langle b_n, c_n \rangle$ ,  $\nu_n = \lambda_n \langle d_n, v_n \rangle$  and  $\rho_n = \mu_n \nu_n - \pi_n^2$ .
8. Set

$$u_{n+1} = \begin{cases} u_n + d_n, & \text{if } \rho_n = 0, \pi_n \geq 0; \\ u_0 + (1 + \frac{\pi_n}{\nu_n}) d_n, & \text{if } \rho_n > 0, \pi_n \nu_n \geq \rho_n; \\ u_n + \frac{\nu_n}{\rho_n} (\pi_n b_n + \mu_n d_n), & \text{if } \rho_n > 0, \pi_n \nu_n < \rho_n. \end{cases}$$

9. Set  $n = n + 1$  and go to step 2.

This algorithm is well adapted to our need since it allows the combination of constraints arising in both the spatial and the wavelet domain. In addition, it has been shown in [13] that this algorithm offers a lot of flexibility in terms of implementation. In particular, several processors can be used in parallel to compute the subgradient projections on the different constraint sets  $(S_i)_{1 \leq i \leq m}$ . For instance, if  $2^{2K}$  parallel processors are available, wavelet based constraints with respect to all possible circular shifts  $s$  in (16) can be processed simultaneously, leading to improved results while reducing the computational time.

## 5. EXPERIMENTAL RESULTS

In this section we evaluate the performance of the proposed method using both synthetic and real data sets commonly found in the stereo literature and exploiting the constrained quadratic minimization method described in Section 4.

### 5.1 Objective function

The objective function is the quadratic term derived from our linearized stereo model (see Section 2). To cope with large deviations from the data model (outliers), occlusion points have been detected and discarded from the summation

in Equation (5). Here, we make use of the uniqueness and ordering constraints to detect the presence of occlusions. For a review of some existing occlusion detection methods, we can refer to [1].

Since  $L$  in (5) is usually not invertible, we introduce the term  $\alpha\|u - \bar{u}\|^2$  to make  $J$  strictly convex, in compliance with the assumption required for the convergence of the proposed algorithm [13]. Denoting  $\mathcal{O}$  the occlusion field and  $\mathbf{x} = (x, y)$  a point in the reference view, the resulting objective criterion is given by:

$$J(u) = \sum_{\mathbf{x} \in \mathcal{D} \setminus \mathcal{O}} [L(\mathbf{x}) u(\mathbf{x}) - r(\mathbf{x})]^2 + \alpha \sum_{\mathbf{x} \in \mathcal{D}} [u(\mathbf{x}) - \bar{u}(\mathbf{x})]^2, \quad (21)$$

where  $\bar{u}$  is an initial estimate and  $\alpha$  is a positive constant that weights the first term relatively to the second. Experiments show that values ranging from 10 to 100 allow to obtain reliable results.

In order to render the approach more robust to outliers, the additive term has to handle with the occlusion problem. It is therefore important to deal with a consistent initial disparity field. In our case, we consider an initialization derived from the left-right consistency constraint. More precisely, using a correlation based method, we compute left-to-right and right-to-left initial disparity maps, denoted respectively by  $\bar{u}_l$  and  $\bar{u}_r$ , and for each point  $\mathbf{x} = (x, y)$  we take  $\bar{u}(\mathbf{x}) = \bar{u}_r(x - \bar{u}_l(\mathbf{x}), y)$ . We then iteratively refine the initial disparity estimate by choosing the result from a previous estimate as the initial value of the next step. We also note that minimizing the functional (21) is equivalent to minimizing (20) where  $R = L^*L + \alpha \text{Id}$  and  $u_0 = R^{-1}(L^*r + \alpha\bar{u})$ .

## 5.2 Constraints

The constraint set arising from the knowledge of the disparity range values is  $S_3 = [u_{\min}, u_{\max}]$ . We note that in practice  $u_{\min}$  and  $u_{\max}$  are often available. For the regularization constraint, we experiment both the Total Variation based constraint and the wavelet based constraints associated to the convex constraint sets  $S_1$  or  $S_2$  (see Section 3). For the choice of the wavelet basis, different families have been tested and it appeared that, when translation-invariant representations are used, Haar wavelets are well-suited for disparity map images with sharp discontinuities.

One of the advantages of the proposed method is to allow a wide range of constraints to be incorporated. To benefit from this advantage, we consider another constraint inspired from the work in [12] that used a regularization term  $(\nabla u)^\top D(\nabla I_L)(\nabla u)$  based on the Nagel-Enkelmann operator [15]. The main idea of this constraint is to attenuate smoothing across intensity edges of the left reference image  $I_L$ . Details given in [12] about this oriented smoothness constraint can help for giving an approximation  $\kappa_4$  of this term leading to the following convex set:

$$S_4 = \{u \in H \mid (\nabla u)^\top D(\nabla I_L)(\nabla u) \leq \kappa_4\}. \quad (22)$$

We remark that the exact projection onto  $S_3$  is straightforwardly obtained whereas a subgradient projection onto  $S_4$  can be easily calculated.

## 5.3 Synthetic Corridor images

In our first experiment, we have tested the proposed approach on the synthetic corridor image pair from the university of Bonn. As the ground truth is available, it is possible to determine the estimation quality quantitatively by computing the Mean Absolute Error between estimated and ground truth disparities. Experiments on both corridor data set

without and with additive zero-mean Gaussian noise of variance  $\sigma_n^2$  have been conducted. The quantitative comparison in Table 1 and the disparity maps in Fig. 1 demonstrate the high-quality results provided by our approach. In particular, one should note that our method is very robust to noise and that our results for the different noise levels are still more accurate than the results of the correlation based approach for the original data set without noise. Fig. 1 shows also that the wavelet based constraints yield better results than the Total Variation one. Another advantage of wavelet based constraints with respect to TV is the computation time. An evaluation on a parallel computing architecture with 8 processors was carried out. This evaluation is much more favorable to wavelet based constraints than the Total Variation: for example, rather than alternating the 4 constraints in (16) with respect to  $s \in \{0, \dots, 3\}^2$  when  $K = 1$ , each one can be assigned to a distinct processor. Fig. 2 shows the value of the normalized Mean Square Error versus the CPU time. The wavelet based method involving the constraint set  $S_2$  is seen to yield a faster convergence.

## 5.4 Real stereo images

Here, we report the results of the application of our approach on standard image pairs available at the Middlebury Stereo Vision website [2]. We also report the results of some state-of-the-art methods from the same website. Table 2 provides a quantitative comparative study using two global error measures: the Root Mean Square error and the Mean Absolute Error. We note that in accordance with [2], we exclude pixels that are in occluded regions when computing the disparity errors. However, as expected and shown on the recovery disparity map (Fig. 3.c), this would not have been necessary for our approach as it yields robust disparity estimates in those points. In order to measure the impact of each constraint, we also indicate in Table 2 the error values obtained when one of the constraints is missing. This confirms that it is useful to incorporate multiple constraints.

## 6. CONCLUSION

In this paper, we have proposed a new wavelet based approach for disparity estimation. Using a convex set theoretic formulation, the original matching problem is translated into that of minimizing a quadratic objective function under convex constraints. Based on wavelet frames, we have investigated an edge-preserving regularization constraint. The resulting optimization problem is solved via a block iterative method that allows to combine both wavelet and spatial domain constraints. Comparison with state-of-the-art methods from the Middlebury Stereo Vision website confirms the high quality of the achieved results.

Table 1: Comparative results on the Corridor stereo pair using the Mean Absolute Error measure.

Technique	noise levels			
	without noise	$\sigma_n^2 = 1$	$\sigma_n^2 = 10$	$\sigma_n^2 = 100$
Correlation method	0.52	0.65	0.99	1.26
TV constraint	0.24	0.29	0.33	0.50
$S_1$ constraint	0.21	0.26	0.30	0.46
$S_2$ constraint	<b>0.19</b>	<b>0.24</b>	<b>0.26</b>	<b>0.41</b>

## REFERENCES

- [1] M. Z. Brown, D. Burschka and G. D. Hager, "Advances in computational stereo," *IEEE Trans. Pattern Anal. Machine Intell.*, vol. 25, pp. 993–1008, 2003.

Table 2: Performance comparison with stereo algorithms from the Middlebury Stereo Vision page [2] for the Map image pair. MAE: Mean Absolute Error, RMS: Root Mean Square error.

Technique	MAE	RMS
Segm+glob.vis.[16]	0.53	2.29
2-pass DP [17]	0.30	1.39
Patch-Based [18]	0.31	1.04
Prop. Meth. ( $S_2 \cap S_3 \cap S_4$ )	<b>0.21</b>	<b>0.96</b>
Prop. Meth. ( $S_3 \cap S_4$ )	0.29	1.37
Prop. Meth. ( $S_2 \cap S_3$ )	0.27	1.24

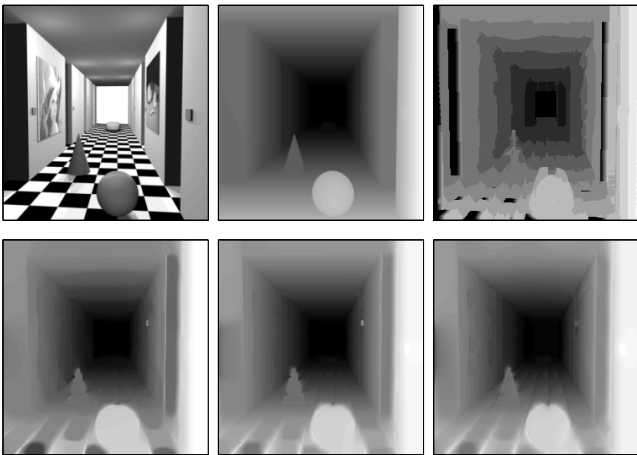


Figure 1: Corridor stereo data set. (Top Left) Reference image. (Top Center) Ground truth. (Top Right) Correlation based. (Bottom Left) TV constraint. (Bottom Center)  $S_1$  constraint. (Bottom Right)  $S_2$  constraint.

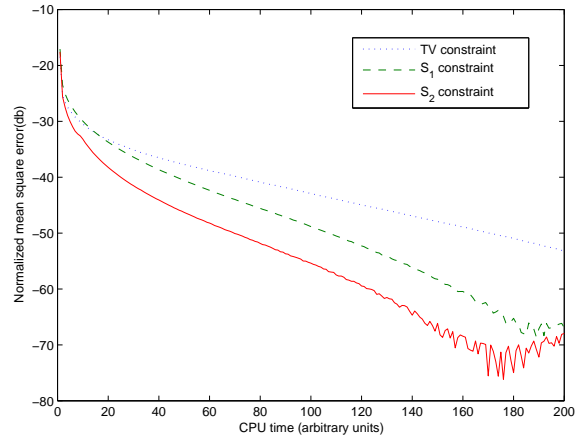


Figure 2: Normalized Mean Square Error versus the CPU time.

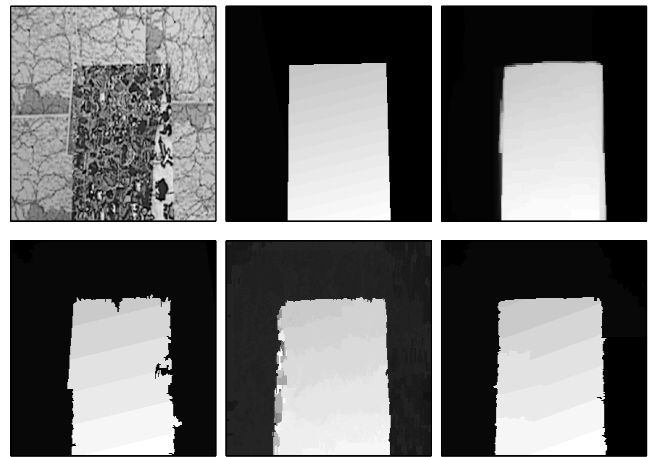


Figure 3: Map stereo data set. (Top Left) Reference image. (Top Center) Ground truth. (Top Right) Prop. Meth. (Bottom Left) Segm+glob.vis. [16]. (Bottom Center) 2-pass DP [17]. (Bottom Right) Patch-Based [18].

[2] D. Scharstein and R. Szeliski, "A Taxonomy and evaluation of dense two-frame stereo correspondence algorithms," *Int. Journal of Computer vision*, vol. 47, pp. 7–42, 2002.

[3] Y. Wu, L. Chen, P. Lee, T. Yeh and J. Hsieh, "Discrete signal matching using coarse-to-fine wavelet basis functions," *Pattern Recognition*, vol. 36, pp. 171–192, 2003.

[4] H. Liu and P. Bhattacharya, "Uncalibrated stereo matching using DWT," *In Proc. Int. Conf. Pattern Recognition*, Vol 1, pp. 114–118, 2000.

[5] Y. S. Kim, J. J. Lee, and Y. H. Ha, "Stereo matching algorithm based on modified wavelet decomposition Process," *Pattern Recognition*, vol. 30, pp. 929–952, 1997.

[6] P. L. Combettes and J. C. Pesquet, "Wavelet-constrained image restoration," *Int. Journal of Wavelets, Multiresolution and Information Proc.*, vol. 2, pp. 371–389, Dec. 2004.

[7] P. L. Combettes and J. C. Pesquet, "Image restoration subject to a total variation constraint," *IEEE Trans. Image Proc.*, Vol. 13, pp. 1213–1222, Sept. 2004.

[8] H. Choi and R. Baraniuk, "Multiple basis wavelet denoising using Besov projections," in *Proc. IEEE Int. Conf. Image Proc.*, pp. 595–599, 1999.

[9] K. P. Horn and G. Schunck, "Determining optical flow," *Artificial Intelligence*, No. 7, pp. 185–203, 1981.

[10] J.-C. Pesquet, H. Krim and H. Carfantan, "Time invariant orthonormal wavelet representations," *IEEE Trans. Signal Processing*, Vol. 44, pp. 1964–1970, Aug. 1996.

[11] J. Weickert, A. Bruhn, N. Papenberg and T. Brox, "Variational Optic Flow Computation: From Continuous Models to Algorithms," *Int. Workshop on Computer Vision and Image Analysis*, 2003.

[12] L. Alvarez, R. Deriche, J. Sanchez and J. Weickert, 'Dense dispar-

ity map estimation respecting image discontinuities: A PDE and scale-space based approach," *Journal of Visual Communication and Image Representation*, Vol. 13, pp. 3–21, 2002.

[13] P.L. Combettes, "A block iterative surrogate constraint splitting method for quadratic signal recovery," *IEEE Trans. on Signal Proc.*, Vol. 51, pp. 1771–1782, Jul. 1997.

[14] S. Mallat, "A theory for multiresolution signal decomposition: The wavelet representation," *IEEE Trans. Pattern Anal. Machine Intell.*, Vol. 11, pp. 674–693, Jul. 1989.

[15] H. H. Nagel and W. Enkelmann, "An investigation of smoothness constraints for the estimation of displacement vector fields from image sequences," *IEEE Trans. on Pattern Anal. Mach. Intell.*, vol. 8, pp. 565–593, 1986.

[16] M. Bleyer and M. Gelautz, "A layered stereo algorithm using image segmentation and global visibility constraints," *Int. Conf. on Image Proc.*, pp. 2997–3000, 2004.

[17] C. Kim, K.M. Lee, B.T. Choi, and S.U. Lee, "A dense stereo matching using two-pass dynamic programming with generalized ground control points," *Computer Vision and Pattern Recognition*, vol. 2, pp. 1075–1082, 2005.

[18] Y. Deng, Q. Yang, X. Lin, and X. Tang, "A symmetric patch-based correspondence model for occlusion handling," *Int. Conf on Computer Vision*, vol. 2, pp. 1316–1322, Oct. 2005.